

# Intrinsic correlation between superconductivity and magnetism

Xiuqing Huang\*

<sup>1</sup>Department of Telecommunications Engineering ICE, Army Engineering University, Nanjing 210007, China

<sup>2</sup>Department of Physics and National Laboratory of Solid State Microstructure, Nanjing University, Nanjing 210093, China

(Dated: March 29, 2023)

Based on the real-space Mott insulator model, it is found that there is a unified pairing, coherent and condensate mechanism of superconductivity for all materials. Partly motivated by Dirac's magnetic monopole and Maxwell's displacement current hypothesis, we demonstrate that electric and magnetic fields are intrinsically relevant. An isolated proton or electron creates an electric field, whereas a real-space quantized proton-electron pair creates a magnetic field. These findings offer new insights into the nature of electron spin, magnetic monopoles, and the symmetry of Maxwell's equations. We argue that the electric dipole vector of the proton-electron pair plays the role of the Ginzburg-Landau order parameter in the superconducting phase transition. It appears that the Peierls transition of the electron-proton electric dipole lattice leads to the symmetry breaking of the Mott insulating state and the emergence of superconducting and magnetic states. Under the new theoretical framework, the Meissner effect, the London penetration depth, magic doping, flux neutralization, vortex lattice, vortex dynamics, and other superconducting phenomena can be consistently explained.

PACS numbers: 71.10. w, 74.20. z, 74.25.Ha, 75.10.-b

## I. INTRODUCTION

Since the discovery of superconductivity in mercury by Kamerlingh Onnes [1], thousands of superconducting elements and compounds have been discovered [2–11]. From a fundamental point of view in the physics community, these superconducting materials can be divided into two classes: conventional and unconventional. It is widely accepted that conventional superconductors can be well described by BCS electron-phonon theory [12], while unconventional superconductors cannot be understood by BCS theory. The boom in superconductivity research started with Bednorz-Muller's remarkable discovery [4]. Following Cooper's pairing picture, physicists have spent thirty-seven years exploring high-temperature superconductivity's mechanism (pairing glue). Even though more than 200,000 theoretical and experimental papers have been published, and hundreds of microscopic theories have been proposed to unravel the mystery based on the rich phase diagram (see Fig. 1) [13–22], none have been considered valid [23]. In the face of such a situation, Anderson strongly challenged the existence of glue responsible for pairing electrons in cuprate superconductors [24].

It seems unconventional that the extensive and intensive research could not make progress in understanding superconductivity. The time has come for the physical community to seriously question whether all our surveys have been misguided by some common sense mistakes. In other words, is it possible that some widely accepted and commonly used theories or models may not capture the essence of the superconducting phenomenon [25, 26]? From a personal point of view, the problem of high-temperature superconductivity is a new dark cloud floating in the physics sky. To solve it, we must first jump out of the old theoretical framework that used to confine our thinking. Furthermore, researchers should no longer waste time and effort entangled in the so-called pairing glue, as suggested by Anderson. However, they should

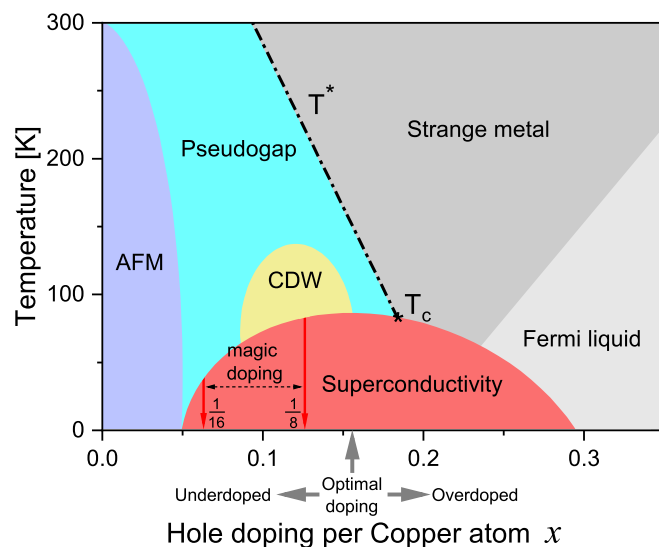


Figure 1: A illustration of hole doped cuprates phase diagram

carefully consider the following fundamental questions.

**First Question:** There are now more than 32 different classes and thousands of superconductors [27]. Nearly all materials and even some insulators can exhibit superconductivity under the right conditions (an appropriate temperature and external pressure). Is it still a good idea to divide superconducting materials into conventional and unconventional superconductors and subjectively assume they have different superconducting origins?

**Second Question:** The zero resistance in an electric field [1] and the Meissner effect in a magnetic field [28] are two critical experimental phenomena observed in all superconducting materials. These experiment facts indicate that any superconductors (whether conventional or not) should share an exact superconductivity mechanism. Moreover, electromagnetic interaction is the most crucial incentive for super-

conductivity. Therefore, the superconducting problem is a simple dynamic problem: how does the external electromagnetic field interact with the charge carriers inside the superconductor and induce the superconducting phase transition?

**Third Question:** From the perspective of the Landau-Ginzburg phase transition theory [29], symmetry breaking occurs in the order parameter characterizing the superconducting phase transition. Hence, it is evident that the superconducting phase transition is not spontaneous but driven by an external field from a high symmetry in the absence of an external field to a lower symmetry in the presence of an external field. Obviously, the key question in the study of the superconductivity mechanism is which electromagnetic variable qualifies as the superconducting order parameter in Landau-Ginzburg's theory.

**Fourth Question:** High-temperature superconductivity in the copper-oxide is commonly believed to originate from an antiferromagnetic parent Mott insulator with the entire range of electron localization and a long-range order [30, 31]. On the one hand, strong magnetic excitations are generally believed to play a vital role in the superconducting mechanism [32–34]. On the other hand, there still remains an unsolved mystery concerning the origin and nature of magnetism. The final solution of high-temperature superconductivity mechanism must be based on the fact that we have successfully explained the fundamental reason of magnetism at the microscopic level. Thus, a pivotal step in explaining superconductivity is to unravel the nature of magnetism and how to elucidate the antiferromagnetic order in a localized electronic framework.

This paper studies these four questions in a unified framework, perfectly revealing the intrinsic relationship between superconductivity, magnetism, order parameters, and symmetry breaking. We show that the magnetic phenomenon in nature comes from the simplest electron-proton pair rather than the electron's motion as the academic community generally agrees. Furthermore, the electron-proton (ion) pairs can self-assemble into an antiferromagnetic Mott insulator by direct electromagnetic interactions of opposites-attraction. We find that the proton-electron electric dipole vector is precisely the order parameter of the Ginzburg-Landau theory of superconducting phase transition. It seems pretty encouraging that the new mechanism can qualitatively and self-consistently explain many important superconducting phenomena, such as the Meissner effect [28, 35], London penetration depth [36], magic doping [37–39], vortex lattice [40–45], and vortex dynamics [46–52]. In addition, our hypothesis can successfully achieve the perfect symmetry of Maxwell's equations [53] and reveal the physical nature of electron spin [54] and Dirac's magnetic monopoles [55].

## II. ARE FREE ELECTRONS FREE?

In 1900, Drude constructed a theory to explain the transport properties of electrons in metals [56, 57]. In 1927, Som-

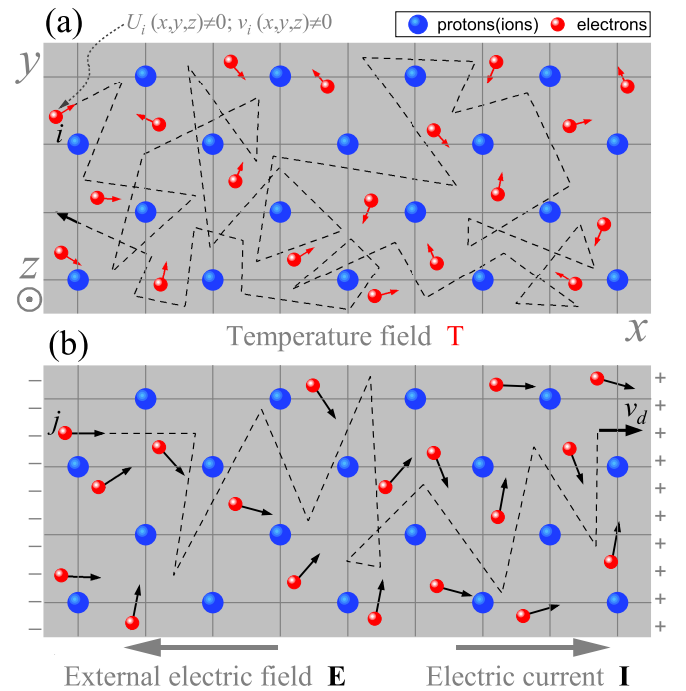


Figure 2: Drude free electron model and conductivity. (a) In the case of temperature  $T > 0$  and no external electric field, the kinetic energy and potential energy of any valence electron in the conductor are not zero; (b) when applied an external electric field  $\mathbf{E}$  on the metal, all electrons move directionally with a drift velocity  $v_d$  to generate an electric current  $\mathbf{I}$ .

merfeld further developed the theory by considering quantum mechanisms [58]. Even though the mathematical forms of the theories look very different, the basic physical concepts have mostly stayed the same. As shown in Fig. 2, the fundamental idea of the theories is based on a simplified model of that lattice of positive immobile ions (for convenience, it can be simplified to protons) and the valence electrons that are free to move about. As shown in Fig. 2(a), without an external electric field, any electron (as the  $i$ -th electron in the figure) will never stop colliding with ions and other electrons in random thermal movement inside the metal. As shown in Fig. 2(b), under an applied electric field  $\mathbf{E}$  along  $-x$  direction, the free electrons will make a random directional motion with a drift velocity  $v_d$  in the opposite direction to conduct an electric current  $\mathbf{I}$ . The collision of electrons with the lattice and other electrons results in resistance.

From an intuitive point of view, Drude's theoretical model is full of contradictions. First, the tortoise's speed of electrons and the light speed of current are a pair of inconsistent contradictions in the Drude hypothesis. Secondly, "Like charges repel each other" is fundamental scientific knowledge, hence, the Drude model has to face a fatal challenge: how can positively charged ions that repel each other form a stable and symmetry crystal structure when electrons are completely disordered? In the following, we will further question the rationality and reliability of the Drude model from the aspects of

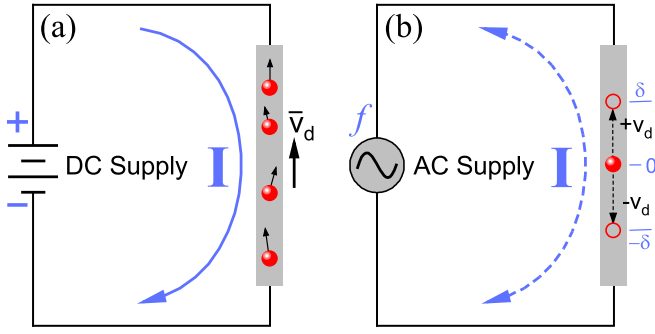


Figure 3: Drude's free electrons are not free. (a) In the case of *DC*, all Drude's electrons flow along the circuit, where electrons are in an extended state. (b) In the case of *AC*, electrons are confined to vibrate back and forth in a small space on the order of angstroms, where the electrons are in a bound state.

current and energy.

As illustrated in Fig. 2(b), we know that the current passing through a conductor follows the equation:

$$I = neS\bar{v}_d, \quad (1)$$

where  $n$  is the charge carrier (electrons) density,  $e$  is the electronic charge,  $S$  is the cross-sectional area of the conductor, and  $\bar{v}_d$  is the average drift velocity.

As shown in Eq. (1) and Fig. 3(a), in the case of steady direct current (*DC*), the magnitude of the current  $I$  and the average drift velocity  $\bar{v}_d$  of the electrons are constant for a given uniform wire. In this case, the conductor has a continuous flow of charge from one point to another, and any electron keeps repeating the circuit cycle.

For the case of alternating current (*AC*) of Fig. 3(b), the current  $I$  periodically reverses itself, and so does the direction of the electron flow. This periodic reversion is a physical impossibility with Drude's free model. Taking  $f = 100$  kHz alternating current as an example, all electrons inside the wire must stop ( $v_d = 0$ ) and change motion-direction at the same period every  $0.01$  ms. It is the fact that electrons have inertia, and their velocities are different in magnitude and direction, as suggested by Drude. Obviously, Drude's free electrons cannot instantaneously respond to the change in the external electric field. The existence of high-frequency alternating current means that the electrons in an *AC* circuit do not move along with the current flow. As shown in the Fig. 3(b), anyone electron is like a harmonic oscillator moving back and forth in its respective equilibrium position "0" with amplitude  $\delta$ . There are two questions: (1) What is the order of magnitude of the amplitude  $\delta$ ? (2) Where are the equilibrium positions of the free electrons in the wire?

For the first question, we know that for copper  $n = 8.5 \times 10^{28}/m^3$ , let us assume a current of  $3A$  that is flowing in a copper conductor with the wire diameter is  $5$  mm, by equation (1) we obtain  $\bar{v}_d \sim 10^{-5} m/s$ . When  $f = 100$  kHz, the amplitude can be estimated as  $\delta < \bar{v}_d/(2\sqrt{2}f) \sim 1\text{\AA}$ . This

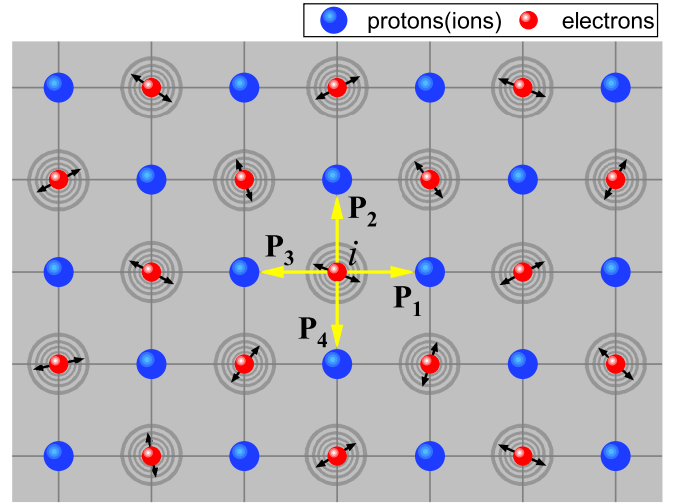


Figure 4: A Mott-insulator-based new electron-crystal model. There are no free electrons inside the material, and the electrons are trapped by the electric field of the surrounding ions (protons) and do thermal vibration in the equilibrium position. When  $T = 0$ , the crystal can be simplified to a symmetric proton-electron pair lattice, exactly the Mott insulator.

result indicates that the alternating current electrons must be localized within a lattice constant. This result is very important since the transmission of alternating current can be realized only by micro displacement of electrons, so should direct current. Then the task is to find the respective equilibrium position for each electron in the metal.

The minimization of the potential energy usually determines the position of equilibrium. Because Drude's free electron model is based on the mean-field approximation, it is evident that the most dominant electron-lattice interactions have been removed, and the potential energy of the electrons is ignored. To answer the second question, we must start with the minimum free energy principle. As shown in Fig. 2(a), the energy of a free electron in a metal consists of two parts, one kinetic due to the free motion  $v_i(x, y, z)$  and the other potential  $U_i(x, y, z)$  provided by the positive ion lattice. Hence, we can define the total free energy of electrons:

$$E_{free} = \sum_i \left[ \frac{m_e v_i^2(x, y, z)}{2} + |U_i(x, y, z)| \right], \quad (2)$$

where  $m_e$  is the mass of the electron.

It is not hard to see from Eq. (2) that when  $v_i(x, y, z) = 0$ , and  $U_i(x, y, z) = 0$ , we immediately have the minimum total free energy  $E_{free} = 0$ . Fig. 4 shows the candidate zero potential energy structure, known as Mott insulators. The most crucial repeating unit is the yellow electron-proton (ion) electric dipole, and the mysteries of nature are hidden inside. In Mott's model, the positively charged ions and negatively charged electrons each form the same sublattice, which is the perfect unity of China's ancient philosophy of complementary "yin and yang" and the principle of minimum energy in mod-

ern western science. The basis of complementarity between “yin and yang” is equal rights, and stable crystals of positive and negative charges must be formed based on mutual equality. In the Drude model, positive and negative charges are unequal and must violate the minimum energy principle.

The Drude model is still used extensively in condensed matter physics teaching and research. In addition to the *AC* issues discussed above, a more severe problem with the Drude model arises when it is extended to describe superconductivity. In the BCS framework, electrons are assumed to flow without resistance in superconductors at low temperatures when paired with opposite spins and momentum. This explanation implies that although the paired electrons are in random motion, they can intelligently avoid electron-lattice and electron-electron collisions, which we consider unscientific. One might ignore the physical mechanism that guarantees the Cooper pairs always keep their spin and momentum opposite. However, no one can ignore the fact that electron-ion attractive interactions and electron-electron repulsive interactions still exist. In particular, the coherence radius of the Cooper pair is much larger than that of a single electron, consequently significantly increasing the collision probability between pair-pair and pair-lattice. Therefore, BCS electron-pairing based on Drude’s free electron postulates can not eliminate the resistance of the superconductors. On the contrary, it dramatically increases resistance.

In addition, as can be seen from Fig. 2(a), it must be directly inferred from the Drude model that the purer the conductor, the smaller its resistance value. Impurities and defects are not conducive to reducing resistance, let alone helping to achieve superconductivity. However, according to the phase diagram of Fig. 1, doping not only does not increase the resistance but makes the resistance mysteriously disappear. Especially in the under-doped region, the more impurities, the higher the superconducting transition temperature. Therefore, there is only one reasonable possibility for this abnormal behavior. That is, the current in the metal wire and the supercurrent in the superconductor do not depend on the directional motion of the electrons. This conclusion is in good agreement with the previous discussion.

Free electrons are not free, and this is undoubtedly a revolutionary idea that will change many essential concepts in physics. It may seem common sense that electricity (or electric current) is an electromagnetic wave that travels at the speed of light and has almost nothing to do with the movement of electrons. The electrons in the wires do not need to carry electrical energy from place to place, as described by Drude’s free electron model. To view this problem more clearly, it is possible to make an analogy with high-speed traffic. Here, wires, electrons, and currents correspond to roads, gates, and moving cars. The gate has two states: open and closed, and electrons also function as switches in the conductor. When the electrons are in the equilibrium position (off), the wire is insulated and non-conductive. The wire changes into a conductive metal state when the electrons leave the equilibrium position (on). In the following sections, we will

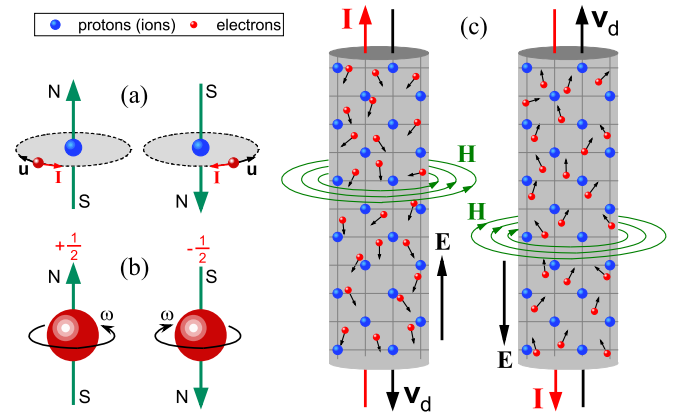


Figure 5: The traditional picture of magnetic fields induced by electron movement. (a) The orbital motion of electrons creates magnetic moments, (b) the electron spin hypothesis, (c) the electrons’ upward and downward directed motion produces counterclockwise and clockwise magnetic fields, respectively.

show in detail how our immobile-electric-charges hypothesis self-consistently explains the phase transition behavior between insulators, metals, semiconductors, superconductors, and magnets.

### III. THE MICROSCOPIC ORIGIN OF MAGNETISM

The first application of magnetism can be traced back to the compass invented by the Chinese more than 2,000 years ago. Modern physics believes that the nature of magnetism lies in the movement of electrons. As shown in Fig. (5), theoretical physicists suggest that electrons can generate magnetic fields through three different types of motion: (a) orbital circulation, (b) rotation, and (c) directional drift. In order to explain how the motion of electrons generates magnetism, various hypotheses and concepts have been developed, including the orbital magnetic moment, molecular current, spin, and current element.

From basic knowledge of electrodynamics, the movement of electrons is usually accompanied by the emission of electromagnetic waves and the loss of their energy. Therefore, to maintain the magnetic field of Fig. 5, there must be a steady stream of external energy to ensure the movement of electrons. On the other hand, we all know that many permanent magnetic materials exist in the universe, and their magnetic field intensity hardly decays. This objective fact is enough to disprove the theoretical hypothesis that the electron’s motion-induced magnetic fields of Fig. 5. Moreover, the duality between the electric and magnetic fields implies that a magnetic field’s generation needs static magnetic charges. Dirac may have been keenly aware of this problem, which inspired him to propose the well-known theory of magnetic monopoles [55]. Are there static magnetic monopoles in nature? This problem not only involves the symmetry of Maxwell’s equations, but also shake the physics building built on the magnetic field

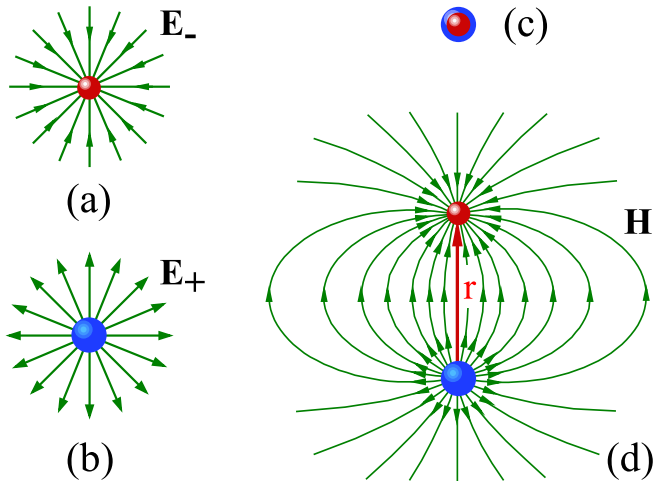


Figure 6: A new magnetic mechanism based on Dirac's theory of magnetic monopoles. (a) and (b) The electric field of an isolated electron and proton, respectively, (c) when the coordinates of the electron and proton coincide, their associated electric fields (or magnetic field) are hidden, (d) an electron-proton pair creates a magnetic field.

generated by moving charges. If magnetic monopoles exist, all our understanding (including Figure 5) of magnetism for thousands of years is wrong. Scientists' theoretical explanations of superconductivity for more than 100 years are also wrong, including BCS theory.

Since Dirac's theory, numerous attempts have been made to find the magical new particles predicted by Dirac. Researchers have not found conclusive evidence of magnetic monopoles for almost a century. There is an ancient poem in China, which means "In the crowd once and again, I look for her in vain. When all at once I turn my head, I find her there where lantern light is dimly shed". So, is it possible that the so-called magnetic monopoles we are trying to find are just another role played by the well-known elementary particles? Below we will provide a possible answer to this question.

Dirac believed that electric and magnetic charge could co-exist and satisfy the following quantization condition:

$$eg = \frac{hc}{4\pi}n = \frac{\hbar c}{2}n, \quad (3)$$

where  $e$  and  $g$  are the electric and magnetic charges, respectively,  $h$  is the Planck's constant [59], and  $n$  being the integers.

What is incredible is that the seemingly simple formula (3) hides the secret of the origin of the magnetism of materials. Using the fine structure constant  $\alpha = e^2/4\pi\epsilon_0\hbar c$ , the Dirac's formula of Eq. (3) can be re-expressed as:

$$g = \left(\frac{n}{8\pi\epsilon_0\alpha}\right)e = \Pi_n e, \quad (4)$$

where  $\Pi_n$  is an adjustable constant.

The above relation of Eq. (4) makes it easy to see that the so-called magnetic monopole is nothing but a dressed electron (or proton), which means that the superimposed electric field created by the electron-proton pair in fact is the magnetic field. Indeed, electrons and protons can play the role of electric and magnetic charges at the same time. Next, we will discuss the generation and annihilation of magnetic fields from the perspective of symmetry breaking.

As shown in Figs. 6(a) and (b), for an isolated electron or proton, they will generate electric fields  $\mathbf{E}_-$  and  $\mathbf{E}_+$  respectively. Assuming that the electron and proton coincide with each other with the spacing  $r = 0$ , as illustrated in Fig. 6(c), due to their perfect symmetry, they neither generate an electric field nor a magnetic field. When  $r \neq 0$ , the electron and proton will form an electric dipole through symmetry breaking, and they will generate a magnetic field strength  $\mathbf{H}$  as shown in Fig. 6(d). It is well known that a changing electric field produces a magnetic field is the most important contribution of Maxwell. When the electric field  $\mathbf{E}_+$  of a positive proton and the electric field  $\mathbf{E}_-$  of a negative electron simultaneously appear in the surrounding space, since the two electric fields are of opposite signs, their superposition represents the changing electric field. Hence, according to Maxwell's hypothesis, the vector superposition of electric fields  $\mathbf{E}_+$  and  $\mathbf{E}_-$  is precisely the magnetic field  $\mathbf{B}$ , which is given by

$$\mathbf{B} = \mu_0\mathbf{H} = \frac{\mathbf{E}_+ + \mathbf{E}_-}{c}, \quad (5)$$

where  $c$  is the speed of light and  $\mu_0$  is the vacuum permeability.

From the above discussion, one can see that in the old framework of Fig. 5(b), the electron spin is considered an intrinsic form of angular momentum [54], which is believed to be a purely quantum mechanical concept. In fact, there is no direct experimental evidence that electrons have spin because whether it is the atomic fine structure experiments [60], or the Stern-Gerlach silver atom beam experiment [61], it can only show that atoms (silver atom or hydrogen atom), not free electrons, have spin magnetic moments. In the new framework of symmetry breaking, it is interesting to note that the conclusion that free electrons have no spin is just hidden in Eq. (5). This formula implies that an isolated electron can only generate an electric field, and there is a non-existent so-called intrinsic spin moment. In atoms, electrons combine with protons to form an electric dipole, as shown in Fig. 6(d), which has the property of magnetic moment and is imagined as electron spin in modern physics. Spin can be thought of as a coat of electrons. Naked electrons have no spin property, so the magical phenomenon of charge-spin separation can be found inside some superconductors.

Accordingly, the question now is how does the new theory explain the magnetic field generated by the current-carrying wire in the surrounding space as shown in Fig. 5(c)? To see why, let us look at Fig. 7, a schematic representation of the generation of magnetic fields solely through the spatial sym-

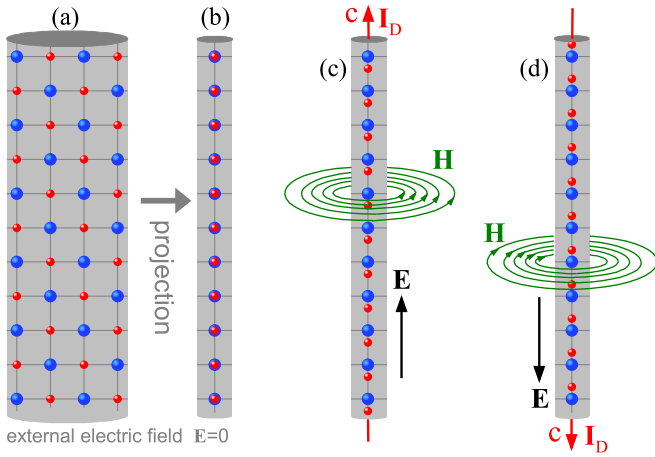


Figure 7: The illustration of how the wire's static electric dipoles generate the magnetic fields. (a) and (b) In the absence of an external electric field and regardless of the influence of temperature, the electromagnetic fields of positive and negative charges are hidden due to the symmetry of the internal structure, so there is no external electric field or magnetic field outside the conductor. (c) and (d) The applied electric field causes the electrons to deviate from the equilibrium position and the symmetry-breaking phase transition, and the upward and downward electric fields will induce counterclockwise and clockwise magnetic fields, respectively.

metry breaking of electron-proton pairs. As shown in Fig. 7(a), in the absence of an external field, the positively charged ions (protons) and electrons inside the wire form a complex lattice structure. For the sake of intuition, it can be projected as a simple quasi-one-dimensional structure of Fig. 7(b), and there is no magnetic field around the wire due to the high symmetry of the electron-proton pairs. As shown in Figs. 7(c) and (d), when an external electric field is applied upwards or downwards along the wire, the electrons in the wire will deviate from the equilibrium position downwards or upwards, respectively, under the action of the electric field. Such Peierls-like symmetry-breaking transition will further induce counterclockwise and clockwise magnetic fields around the wire, as illustrated in the figure.

It is well known that a proton-electron pair is not just an electric dipole, it can also be a hydrogen atom or a neutron. In metal wires, proton-electron pairs are the smallest quantized capacitance in nature, and their capacitance can be determined by  $C_r = 2\pi\epsilon_0 r$  (where  $r$  the distance of the electric dipole). External factors such as temperature and external electric field can make the electromagnetic field energy stored in them release in the form of electromagnetic waves traveling at the speed of light  $c$ . These energies may be the light quanta of blackbody radiation discovered by Planck or Maxwell's displacement current  $\mathbf{I}_D$  as indicated in Figs. 7(c) and (d).

We now have two distinct origins of magnetism, the old explanation relying entirely on the time-dependent persistent movement of electrons and the new explanation being determined by the time-independent electron-proton electric dipole. From the previous analysis and according to the

principle of minimum energy, we can conclude that the idea that the perpetual motion of electrons generates a magnetic field has no scientific basis. This paper's proton-electron pair magnetism mechanism developed from Dirac's magnetic monopole and Maxwell's displacement current hypothesis is likely the more reasonable choice in nature.

#### IV. SYMMETRY OF MAXWELL'S EQUATIONS

The differential form of the Maxwell's equations can be written as:

$$\begin{aligned}\nabla \cdot \mathbf{E} &= \frac{\rho_e}{\epsilon_0}, \\ \nabla \cdot \mathbf{B} &= 0, \\ \nabla \times \mathbf{E} &= -\frac{\partial \mathbf{B}}{\partial t}, \\ \nabla \times \mathbf{B} &= \mu_0(\mathbf{J}_D + \mathbf{J}_e).\end{aligned}\quad (6)$$

where  $\mathbf{E}$  is the electric field,  $\mathbf{B}$  is the magnetic field,  $\rho_e$  is the electric charge density,  $\mathbf{J}_e$  is the electric current density, and  $\mathbf{J}_D = \epsilon_0 \partial \mathbf{E} / \partial t$  is the displacement current.

Maxwell's equations of Eq. (6) is considered the most beautiful and elegant formula in physics. Because it is not mathematically perfect symmetry, significant efforts have still been made to achieve the exact symmetry of the equations, including Dirac's magnetic monopole hypothesis [55]. It should be pointed out that it is not the right way to realize the symmetry of the equation through mathematical skills or artificial hypotheses of new particles. In the previous section, we have obtained three significant findings: (I) the conduction current that relies on the movement of electrons does not exist, (II) the magnetic field is produced by the proton-electron electric dipole of Eq. (5), (III) the magnetic monopoles of Eq. (4) are the isolated electrons and protons.

With the above new findings, we can now reconsider the symmetry of Maxwell's Equations. Maxwell's first equation of Eq. (6) is based on Gauss' law, which describes the electrostatic field. The second equation of Eq. (6) is based on Gauss's law on magnetostatics. Here, we will show that these two equations are intrinsically related, and the second equation can be derived from the first equation. For a proton-electron pair with the electric dipole vector  $\mathbf{P}$ , according to the first equation of Eq. (6), the electric field generated by the pair satisfies:

$$\nabla \cdot (\mathbf{E}_+ + \mathbf{E}_-) = \frac{[\rho_e(\mathbf{r}_p) + \rho_{-e}(\mathbf{r}_p + \mathbf{P}/e)]}{\epsilon_0}, \quad (7)$$

where  $e$  is the electron charge,  $\mathbf{r}_p$  is the coordinate position of the proton,  $(\mathbf{E}_+, \rho_e)$  and  $(\mathbf{E}_-, \rho_{-e})$  are the electric fields and the electric charge densities of proton and electron, respectively.

Substituting Eq. (5) into Eq. (7), we have

$$\nabla \cdot \mathbf{B} = \frac{[\rho_e(\mathbf{r}_p) + \rho_{-e}(\mathbf{r}_p + \mathbf{P}/e)]}{c\epsilon_0}. \quad (8)$$

Usually,  $\mathbf{P}/e$  is an infinitesimal length (far less than an Ångström), under a far-field approximation  $\mathbf{r}_p + \mathbf{P}/e \simeq \mathbf{r}_p$ , it is reasonable to assume that proton and electron nearby of each other, or  $\rho_e(\mathbf{r}_p) + \rho_{-e}(\mathbf{r}_p + \mathbf{P}/e) \simeq 0$ , then Eq. (8) will approximately become the second Maxwell's equation. This result means that Maxwell's second equation is not strictly true, or the right-hand side of the equation is not exactly zero. Furthermore, our conjecture has ruled out the existence of conduction currents, this means that  $\mathbf{J}_e$  in the fourth Maxwell equation must be equal to zero. So far, we have developed all the tools necessary to rewrite the Maxwell equations. The new equations can be given immediately as:

$$\begin{aligned} \nabla \cdot \mathbf{E} &= \frac{\rho_e}{\varepsilon_0}, \\ \nabla \cdot \mathbf{B} &\simeq 0, \\ \nabla \times \mathbf{E} &= -\frac{\partial \mathbf{B}}{\partial t}, \\ \nabla \times \mathbf{B} &= \mu_0 \varepsilon_0 \frac{\partial \mathbf{E}}{\partial t}. \end{aligned} \quad (9)$$

Compared Eq. (9) with Maxwell's equations of Eq. (6), the new equation above has two important breakthroughs. First, one can find the original first and second equations of Eqs. (6) are completely independent and uncorrelated, so strictly speaking, Maxwell's equations have not achieved the unification of electrical and magnetic phenomena. Nevertheless, the new first and second equations of Eq. (9) are intrinsically closely related, the first equation describing the electric field generated by unpaired charges (protons or electrons), and the second equation describing the magnetic field generated by paired charges. Second, due to the existence of excess conduction current  $\mathbf{J}_e$ , the original third and fourth equations of Eq. (6) do not satisfy symmetry. Without the conduction current, the symmetry of the new third and fourth equations is naturally realized.

## V. ANTIFERROMAGNETISM, ORDER PARAMETERS AND MAGIC DOPING

The antiferromagnetic Mott insulator has attracted particular attention because of its potential for unraveling the mystery of high-temperature superconductivity. In the past few decades, the dominant theoretical explanation of high-temperature superconductivity has relied on the Hubbard and extended Hubbard models [21, 22, 62]. It must be pointed out that these models are based on a misunderstanding of the nature of magnetism and antiferromagnetism. So the problem of why Mott insulators have strong antiferromagnetic correlations still needs an explanation. According to the proton-electron paired magnetic dipole hypothesis proposed in this paper, this question is no longer a mystery.

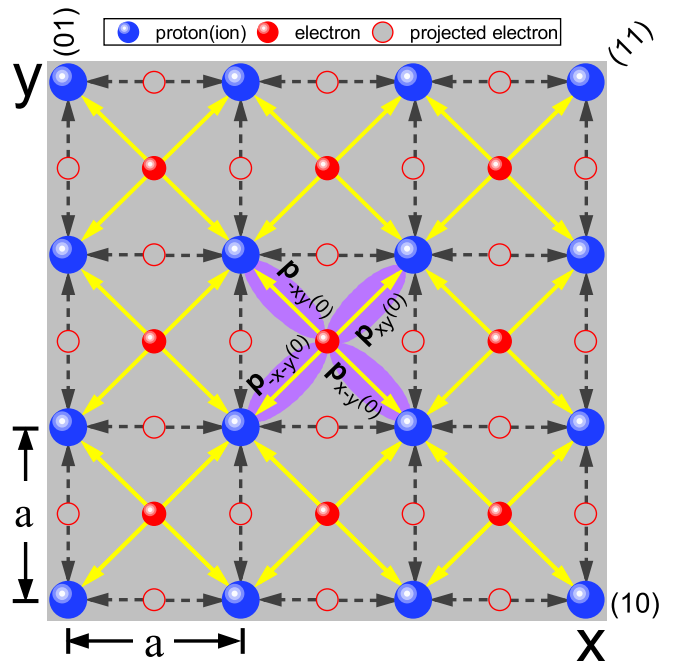


Figure 8: Long-range antiferromagnetic Mott insulator and ground-state electrons with kinetic energy, potential energy, and total energy are all zero.

### A. Mott insulator and ground-state electrons

The electrons in a Mott insulator can be considered identical particles in the ground state. As shown in Fig. 8, we present a two-dimensional Mott insulator phase with square symmetry. Considering only the nearest neighbor pairing, the proton-electron pairs (yellow arrows in the figure) can naturally form antiferromagnetic order along two diagonal directions. For the (10) and (01) directions, the antiferromagnetic order can be characterized by the projected black dashed arrows in the figure. Taking the electron in the center of the figure as an example, we can use four degenerate electric dipole vectors to describe it. These four electric dipoles can be integrated into a total vector as:

$$\begin{aligned} \mathbf{P}_G &= \mathbf{P}_{Mott} \\ &= \mathbf{P}_{xy}(0) + \mathbf{P}_{-xy}(0) + \mathbf{P}_{x-y}(0) + \mathbf{P}_{-x-y}(0) \quad (10) \\ &= 0. \end{aligned}$$

It can be seen directly from Figure 8 and Eq. (10), the Mott-insulating ground state electrons have the following characteristics: (1) it is a stable coherent condensed state with the minimum zero energy; (2) the crystal of negatively charged electrons has the exact symmetry as the crystal of positive ions; (3) the total electric dipole vector of the electron is zero.

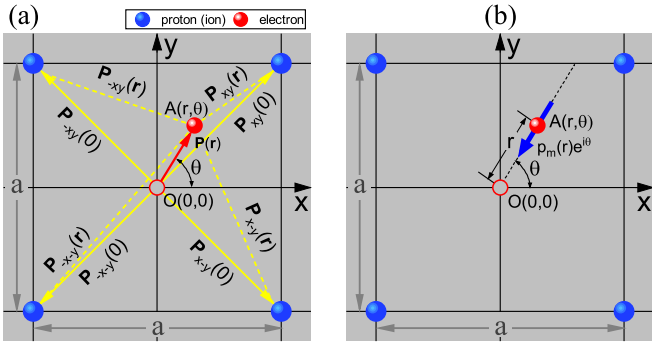


Figure 9: Excited-state electrons in the real-space nearest neighbor interaction approximation. (a) The excited-state electron has a higher energy and a non-zero electric dipole vector  $\mathbf{P}(\mathbf{r})$ . (b) The electron of Fig. 9(a) can be simplified by a magnetic vector  $p_m(\mathbf{r})e^{i\theta}$ .

### B. Excited-state electrons

Under external fields, temperature or pressure, the ground state electrons in Fig. (8) will deviate from the equilibrium position and enter the excited state. Correspondingly, the Mott-insulating state will transition into a metallic, magnetic or superconducting state according to external conditions.

As shown in Fig. 9(a), when the electron occurs transition from ground state  $O(0,0)$  to excited state  $A(r, \theta)$  with a vector  $\mathbf{P}(\mathbf{r})$  marked by the red arrow, the corresponding electric dipole vector  $\mathbf{P}_E$  can be expressed as the superposition of four new electric dipole vectors (the yellow dotted arrows). Using formula (10), we can get the following relationship:

$$\begin{aligned} \mathbf{P}_E &= \mathbf{P}_{xy}(\mathbf{r}) + \mathbf{P}_{-xy}(\mathbf{r}) + \mathbf{P}_{-x-y}(\mathbf{r}) + \mathbf{P}_{x-y}(\mathbf{r}), \\ &= \mathbf{P}_G - 4\mathbf{P}(\mathbf{r}), \\ &= -4\mathbf{P}(\mathbf{r}). \end{aligned} \quad (11)$$

Assuming that the positive ion lattice has not changed before and after the phase transition, the physical quantity  $\mathbf{P}_E$  of Eq. (11) is only related to the change vector  $\mathbf{P}(\mathbf{r})$ . In this case, the physical system of Fig. 9(a) can be simplified as Fig. 9(b), where the  $\mathbf{P}_E$  can be completely endow to the electrons with the intrinsic quantized magnetic vector:

$$\mathbf{P}_m = \Gamma(c, h)\mathbf{P}_E = p_m(\mathbf{r})\exp(i\theta), \quad (12)$$

where  $\Gamma(c, h)$  is the proportional constant related to the speed of light  $c$  and Planck constant  $h$ .

The magnetic vector  $\mathbf{P}_m$  emerges because the superconducting parent's hidden magnetic state is excited. This elementary excitation process is bound to be accompanied by the destruction of the long-range antiferromagnetic phase. The magnetic vector can play the role of spin and magnetic moment of the excited electrons. It is also the physical origin of Planck's quantum theory of radiation, flux quantization, and the quantum Hall effect. Furthermore, it is exactly the order parameter of the Ginzburg-Landau phase transition theory. Obviously, the magnetic properties of electrons are not inherent but come from the combination with positively charged

lattices. Once electrons leave the material and become free, their magnetism (spin) will disappear immediately. It can now be confirmed that electrons do not possess the so-called intrinsic spin, which is why the phenomenon of charge-spin separation can be found in experiments [63].

### C. Order parameters and symmetry breaking

It is without a doubt that the Ginzburg-Landau phase transition theory is the most successful theory of superconductivity so far [29]. As a phenomenological theory, it captures the two primary elements of superconducting phase transition: the order parameter and symmetry breaking. Of course, Landau's theory needs to be completed because it cannot answer the key question on the microscopic level: what is the order parameter with electromagnetic properties? Now, it should be pretty sure that the order parameter in Ginzburg-Landau's theory originates from the proton-electron electric dipole moment as proposed in our theory.

In condensed matter physics, phase transitions in materials are responsible for the changes in their physical properties, which are described through the evolution of a symmetry-breaking order parameter. Since the proton-electron electric dipole can play a vital role in the order parameter, as the most basic requirement, it must provide a unified microscopic explanation for the phase transitions of superconductivity, insulation, magnetic, metallic, etc. For a conductor containing  $N$  valence electrons, from Eq. (12), we can define the order parameter of the conductor as follow:

$$\mathbf{P}_{order} = \sum_{j=1}^N p_m(r_j)\exp(i\theta_j) \quad (13)$$

By using Eq. (13), it is possible to distinguish among five typical condensed states and display their essential differences at the microscopic scale. First, as shown in the Fig. 10(a), when  $r_j = 0$ , then  $p_m(r_j) = 0$  and the order parameter  $\mathbf{P}_{order} = 0$ , this is the insulating state in which no symmetry breaking occurs, and the symmetry of the electrons exactly matches the symmetry of the lattice. In the second case of Fig. 10(b),  $r_j$  is a small random displacement of the  $j$ -th electron from its equilibrium as a result of random thermal fluctuations. Since the orientation order parameter  $\theta_j$  is isotropic, from Eq. (13) we immediately have  $\mathbf{P}_{order} = 0$ . It must be pointed out that although the order parameter  $\mathbf{P}_{order}$  in Figs. 10(a) and (b) are both equal to zero, their corresponding physical systems are entirely different, the former is an insulating state and the latter is a normal state (or disordered state).

Fig. 10(c) shows the third case of the metallic state. Suppose the external electric field is applied alone  $x$  axis, all electrons will collectively shift from around the equilibrium positions to the left. Due to the influence of random thermal motion, the system is non-completely broken symmetry. In this case, the dominated component of the order parameter appears in the  $x$ -direction of the electric field. As a result,

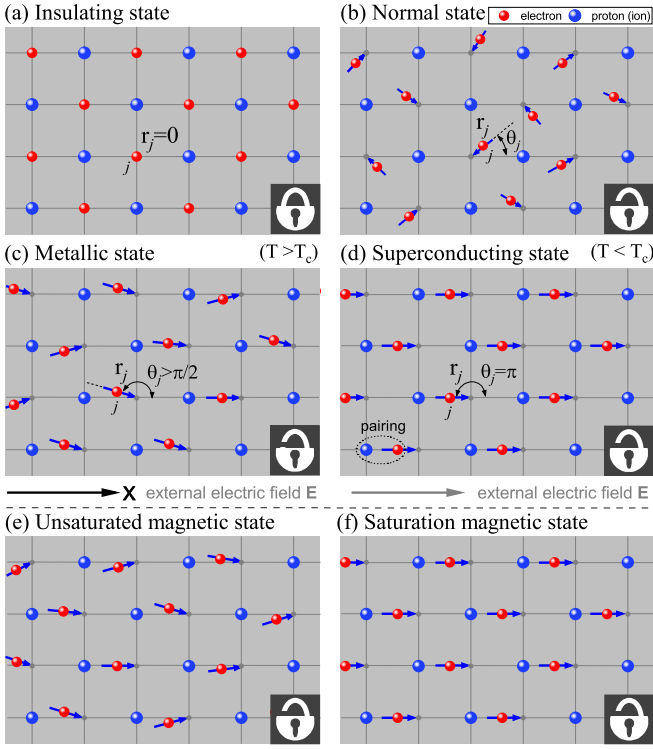


Figure 10: Five typical condensation states based on symmetry and symmetry-breaking. (a) The insulating state with the highest symmetry of perfect crystal; (b) the normal state with a complete disorder of magnetic vector orientation; (c) when  $T > T_c$ , the external field-induced metallic state associated with quasi-parallel magnetic vectors; (d) when  $T < T_c$ , all magnetic vectors are aligned strictly along the direction of the electric field, they become coherent and condense into a quantum superconducting state; (e) and (f) the unsaturated and saturated magnetic states respectively, which may be spontaneous or induced by external magnetic fields. Note that in the case of an insulating state (a), the electrical and magnetic properties of materials are locked (hidden) because of symmetry. When symmetry is broken, the electromagnetic properties will be unlocked and excited.

in addition to the main electromagnetic energy flow in the  $x$ -direction characterized by an electric current. There is energy loss in the direction perpendicular to the electric field, which contributes to the resistance. Figure 10(d) depicts the fourth case of the superconducting state when  $T < T_c$ , the thermal disturbance is almost completely suppressed, and the order parameter is strictly along the direction of the electric field. In this case, the orientation angle in Eq. (13) is the same as  $\theta_j = \pi$ , the system has perfect symmetry breaking, and all electrons condense coherently into a single quantum state with a zero resistance. It should be noted that there is no distinction between conventional and unconventional superconductors under our theoretical framework. The stability of the order parameter  $\mathbf{P}_{order}$  mainly determines the superconducting transition temperature. Because the lattice constant of elementary superconductors is relatively small, the strong repulsive interaction between electrons leads to the instability

of the order parameter  $\mathbf{P}_{order}$ , which in turn makes  $T_c$  lower. In contrast, the lattice constant of high-temperature superconducting materials is generally large and  $\mathbf{P}_{order}$  is much more stable than that of low-temperature superconductors. Furthermore, high pressure can influence the superconducting transition temperature, and the pressure effect on the  $T_c$  can be positive or negative. These experimental results can also be qualitatively explained in Fig. 10(d). On the one hand, pressing reduces the lattice constant, which leads to a decrease in  $T_c$ , on the other hand, it increases the stability of the whole lattice and improves  $T_c$ . Hence, the pressure effect on superconducting properties involves the competition of two distinct structural phase transitions.

Apart from the four states mentioned above, the magnetic state is another essential natural phenomenon closely related to the metallic and superconducting states. Figures 10(e) and (f) show unsaturated and saturated magnetic states, respectively, and their microstructures are entirely consistent with those of metallic and superconducting states of Figs. 10(c) and (d), respectively. The only difference between them lies in the external temperature, electric field, and magnetic field that induce the phenomenon. Our theory suggests that there are three primary types of related complete symmetry breaking phenomena of electronic states in nature exist. The first type is the superconducting state of Fig. 10(d) induced by the combination of electric field and temperature, the second type is the magnetic state of Fig. 10(f) induced only needs to be lowered to a proper temperature (the Curie temperature), and the third type is the superconducting Meissner effect induced by the combination of magnetic field and temperature. It must be emphasized that the micro-physical mechanisms of these three seemingly completely different phenomena are precisely the same, all due to the symmetry breaking of electronic structure related to Peierls phase transition. Permanent magnet materials are spontaneous symmetry breaking phase transitions, while superconductivity is a symmetry breaking phase transition driven by an external field. In particular, our theory shows that superconductivity is a local pairing of electrons and protons (ions) in real space as indicated in Fig. 10(d), which is utterly different from the non-localized  $k$ -space picture of Cooper pairing hypothesized by BCS theory.

Recall Fig. 1 again, the typical phase diagram of copper oxide high-temperature superconductor is complicated. It contains almost all the main phenomena studied by solid-state physics. From the discussion in this section, we can draw an important conclusion that the Mott insulator is the parent of all superconductors, as well as metals, magnets, and semiconductors. From the microscopic point of view, the main difference among different physical phases in the phase diagram Fig. 1 lies in the difference in the orientation order of the electric dipole composed of electrons and protons (ions).

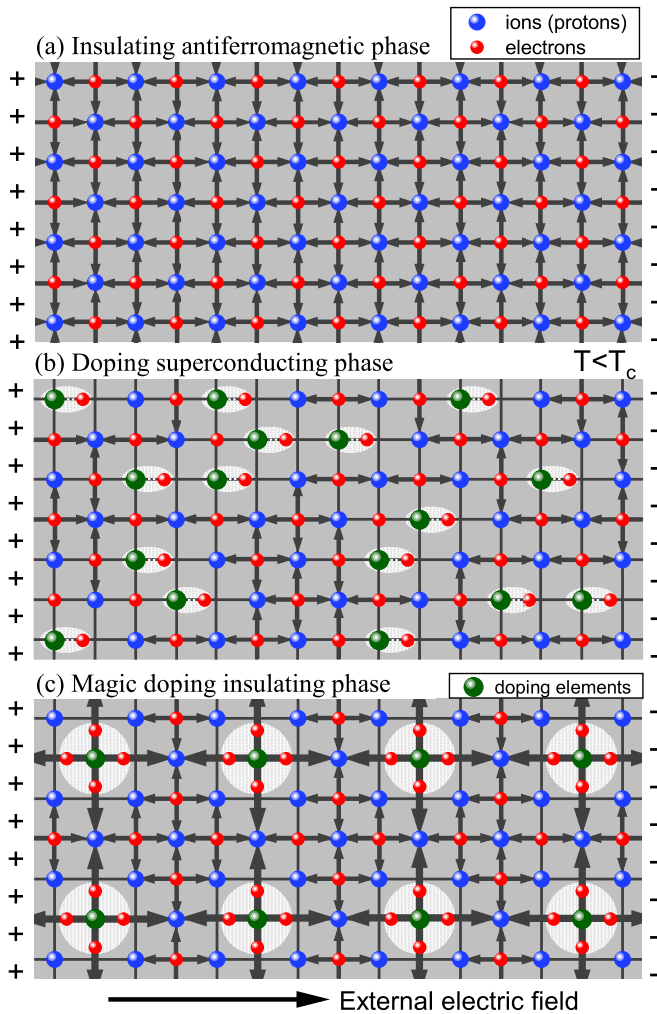


Figure 11: Comparison between cuprate high-temperature superconducting state and magic doping insulating state. (a) The parent Mott insulator with antiferromagnetic order; (b) the doped superconducting state where the long-range antiferromagnetic order is destroyed; and (c) the insulating chessboard structure at the magic doping, where the antiferromagnetic order remains after renormalization.

#### D. Magic doping and chessboard structure

Most of the known cuprate superconductors contain three stable phases: the insulating antiferromagnetic phase, the superconducting phase, and the metallic phase, depending on the concentration of doped carriers. In some cuprate compounds such as  $La_{2-x}Sr_xCuO_4$  (LSCO),  $Ca_{2-x}Na_xCuO_2Cl_2$  (NCCOC), and  $Bi_2Sr_2CaCu_2O_{8+\delta}$  (BSCCO), there exist some charge-ordered states that have been observed to compete with superconductivity. The theoretical studies predict that the 2D chessboard charge ordering patterns can be found at the magic doping fraction  $x = x(m, n) = (2m + 1)/2^n$ , where  $m$  and  $n$  are integers [39].

The experimental fact that localized electron competition phases exist below the superconducting transition tempera-

ture is enough to shake the foundations of the traditional superconducting theory. In the following, we will directly use the magic doping results to re-question the rationality of electron Cooper pairing and resistive superconducting current recognized by superconducting scholars. We can prepare three LSCO superconducting samples, which are  $x = 0.124, 0.125,$  and  $0.126$ , respectively. All three samples are cooled below  $T_c$ , and the experimental results will show that the first and third samples are superconducting while the second is not. Why is superconductivity so sensitive to the change in doping concentration? Obviously, the old superconducting pairing mechanism cannot explain this phenomenon at all. As a newly established superconducting theory in this paper, it must first be able to explain these exceptional cases of magic doping.

Both the antiferromagnetic Mott insulating phase and the magic doping insulating phase suggest that the superconducting mechanism must be established on the basis of a localized electronic picture, as discussed in the above sections. As shown in Figure 11, our theory gives the evolution process of microscopic electronic states of cuprate superconductors from parent insulating state to doped superconducting state and then to magic doping insulating state. For the undoped Mott parent compound of Fig. 11(a), due to the strong electron-ion coupling, the external electric field cannot cause the displacement of electrons, and the symmetry breaking of the order parameters sample remains the long-range antiferromagnetic insulating state. When ions are partially replaced and carriers are randomly doped, as shown in Fig. 11(b), the combination of some local electrons and ions will be significantly weakened. In this case, these electrons will be displaced under the action of the external field, resulting in symmetry breaking and the emergence of superconductivity. In the case of magic doping of Fig. 11(c), some of the ions are replaced regularly with a chessboard structure, and locally symmetric electronic states are formed around ions. The system still retains the long-range antiferromagnetic order after renormalization. Hence the external electric field cannot realize superconducting phase transition by destroying the symmetry of electronic states.

#### VI. MEISSNER EFFECT PUZZLE

In addition to the property of exactly zero resistivity, superconductors are also characterized by the property of perfect diamagnetism, which is known as the Meissner effect [28]. It is generally believed that when a superconductor is placed in a weak external magnetic field  $\mathbf{H}$ , the magnetic field is expelled from the interior if it is cooled below its transition temperature. It must be pointed out that this schematic diagram and explanation, which is widely used in textbooks and papers, is incomplete and may lead to a misunderstanding of the experimental facts.

The magnetic field expelled picture of Fig. 12 shows that the Meissner effect is a time-dependent dynamic process.

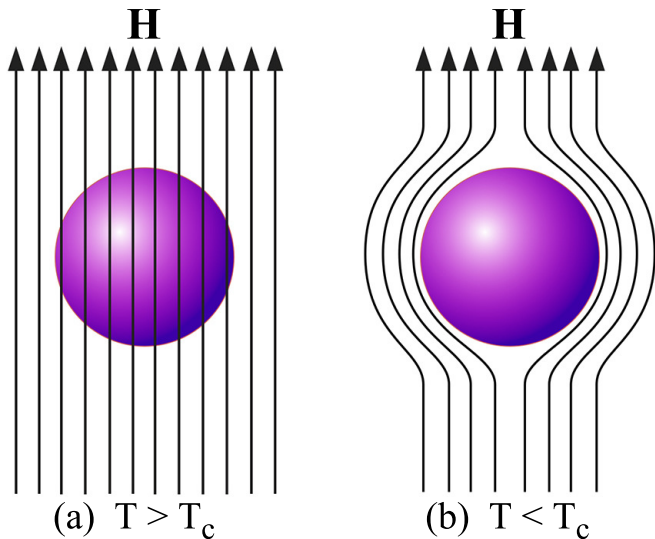


Figure 12: Mainstream explanation of the Meissner effect: (a) above the critical temperature, the magnetic field can pass through the superconductor, (b) below the critical temperature, the magnetic field is excluded from its interior.

Hence, any valuable theory of superconductivity must be able to explain how the superconductor goes from the normal to the superconducting state by expelling the magnetic field against Faraday's law. Almost ninety years have passed since the first experiment conducted by Meissner and Ochsenfeld [28], and many theories and mechanisms have been proposed to explain the Meissner effect. As Hirsch argued [25], these mechanisms have not consistently described the Meissner experiment. In this study, we will solve this puzzle only using the microscopic mechanism of proton-electron electric dipole pairing.

Before starting the following investigation, it is vital to look at the experiment of the Meissner effect [35]. Figure 13 shows two screenshots of the experiment, clearly showing that the superconductor and the magnet can both repel as shown in Fig. 13(a) or attract as shown in Fig. 13(b) each other. Moreover, repulsion and attraction can be switched instantaneously. One can immediately find that the most widely accepted magnetic field expulsion mechanism of Fig. 12 (b) cannot explain the experimental fact that the superconductor and magnet of Fig. 13(b) are attracted to each other. In order to better explain the Meissner effect, we make a force analysis on the magnetic suspension in Fig. 13 (a) and the superconductor suspension in Fig. 13(b), respectively. By assuming that the masses of the magnet and the superconductor are  $m$  and  $M$ , respectively, thus the repulsive force  $F_R$  and the attractive force  $F_A$  satisfy:

$$F_R = mg; \quad F_A = Mg, \quad (14)$$

where  $g$  is the acceleration of gravity.

The above force balance condition of Eq. (14) seems simple but contains important information about the Meissner effect. First, the Meissner effect is directional. Its direction can be automatically adjusted according to the movement trend, mak-

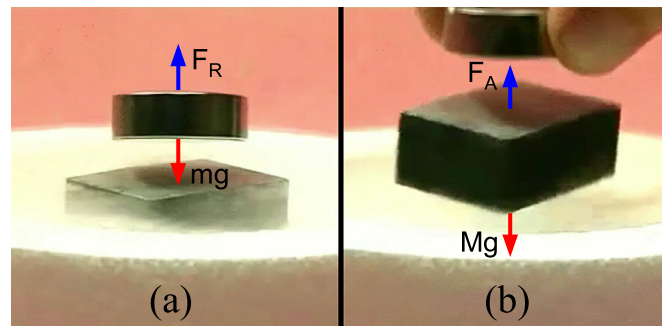


Figure 13: The experiment of Meissner effect: (a) strong repulsion between superconductor and magnet makes the magnet levitate, (b) strong attraction between superconductor and magnet makes superconductor levitate.

ing the magnet and the superconductor attract or repel each other. Second, according to Eq. (14), the Meissner effect can also automatically modulate its strength to balance gravity according to the mass of the magnet or superconductor. This experiment's result is the biggest challenge for theoretical superconductivity researchers. From the perspective of energy conservation, maintaining a stable levitation requires stable external energy input. In the Meissner effect experiment of Fig. 13, the magnetic field is the only external factor outside the superconductor. Hence, it must also be the only source of the force of the levitation phenomenon.

Our theory as a new mechanism of superconductivity, its reliability and consistency must be strictly tested by the experiment results of Fig. 13. As shown in Fig. 14(a), in the absence of an external magnetic field and a temperature below the superconducting critical temperature, all valence electrons will rest at a position with zero potential energy of the Mott phase. When a magnet ( $\mathbf{H}_{\text{ext}}$ ) is placed over a superconductor as shown in Fig. 14 (b), due to the gravitational field, the magnet tends to fall to increase the strength of the magnetic field within the superconductor. Then the electrons will move down from their equilibrium positions, resulting in an induced magnetic field ( $\mathbf{H}_{\text{ind}}$ ) in the opposite direction and a repulsive interaction between the magnet and the superconductor. Thus in the experiment of Fig. 13(a), we could observe the magnet levitating after being repelled by the superconductor. As shown in Fig. 14(c), when the magnet is lifted up from the vicinity of the superconducting surface, gravity will tend to separate the magnet and superconductor, consequently reducing the magnetic field strength inside the superconductor. To resist the process, the electrons in superconductors will move up from their original positions and simultaneously excite an induced magnetic field ( $\mathbf{H}_{\text{ind}}$ ) in the same direction as  $\mathbf{H}_{\text{ext}}$ . Since the net charges on the nearest neighboring surfaces of the magnet and superconductor are of different signs, mutual attraction naturally occurs between them.

From our explanation above, the nature of the Meissner effect is not mysterious. It is merely a simple magnetic interaction between a magnetized superconductor and a mag-

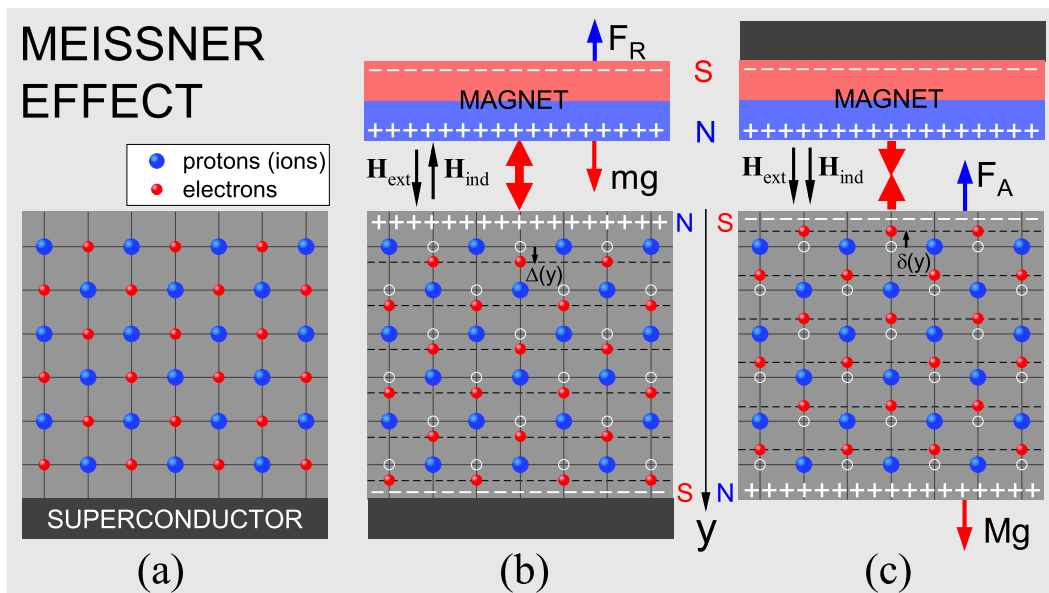


Figure 14: Schematic explanation of Meissner effect experiment of Fig. 13. (a) Without an external magnetic field, the superconductor is the Mott insulator with high symmetry; (b) the magnet above causes the collective displacement of electrons  $\Delta(y)$  in  $y$  direction, then the surface charge on the upper side of the superconductor has the same sign as the lower side of the magnet, resulting in a repulsive interaction; (c) the symmetry breaking occurs due to the collective displacement of electrons  $\delta(y)$  in  $-y$  direction, in this case, the surface charge on the upper side of the superconductor is of the opposite sign to the lower side of the magnet, resulting in an attractive interaction.

net. They follow the fundamental principle of "two identical poles repel and two opposite poles attract." Is there repulsion or attraction between magnet and superconductor? It depends entirely on whether the electrons in the equilibrium position are downward or upward. Furthermore, according to Eq. (14), why is the levitation force ( $F_R$  or  $F_A$ ) automatically adjustable? This question is related to the London penetration depth and will discuss in the next section.

Before concluding this section, we want to briefly say something about the issue of persistent current in superconducting rings. The scientific community generally believes that experiments have repeatedly confirmed the existence of a never-disappearing current in the superconducting circular loop. Some researchers even estimate that the current in the ring will take 100 billion years to disappear completely. Of course, this is just a science fiction story. As basic electromagnetic knowledge, even in the case of vacuum and absolute zero temperature, electrons moving in a circle will lose their energy. The new theory in this paper shows that there is no so-called superconducting current in the superconducting ring, and the magnetic field measured in the experiment is just the magnetic field generated by the electron-proton electric dipoles in the superconducting ring. Strictly speaking, the superconducting ring is a low-temperature magnet induced by the Meissner magnetization effect.

## VII. LONDON PENETRATION DEPTH AND LEVITATION

The strength of the Meissner effect is usually described in terms of  $\lambda_L$ , which is according to the following formula [36]:

$$\mathbf{H}(x) = \mathbf{H}_0 e^{-x/\lambda_L}, \quad (15)$$

where  $\mathbf{H}_0$  is a weak external magnetic field,  $\mathbf{H}(x)$  is the decaying magnetic field inside the superconductor. The London penetration depth is given by

$$\lambda_L = \sqrt{\frac{mc^2 \epsilon_0}{n_s e^2}}, \quad (16)$$

where  $n_s$  is the density of superconducting electrons.

It should be pointed out that the theoretical values predicted by Eq. (16) are not consistent with the experimental results. A large number of experimental results show that the penetration depth is not only closely related to the external magnetic field strength [64] and temperature [65, 66], but also related to the shape, size and orientation of superconducting samples. However, Eq. (16) does not provide the internal relationship between penetration depth, temperature, and magnetic field. In essence, London's theory is just phenomenological, which cannot dynamically explain how the magnetic field enters the superconductor and how it is expelled from the superconductor, let alone clarify the mechanisms of competition among temperature, magnetic field, and penetration depth. Since our present proton-electron electric dipole superconductivity theory is microscopic, it may allow us to study the dynamic processes of London's penetration depth.

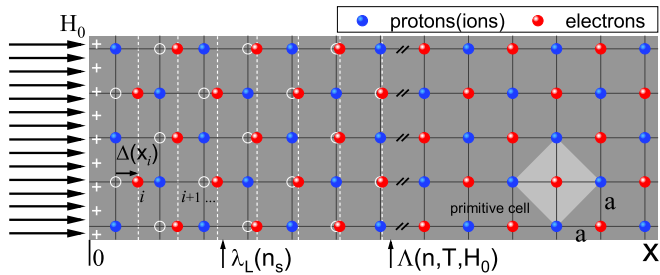


Figure 15: Microscopic explanation of London penetration depth. When the magnetic field  $\mathbf{H}_0$  enters the superconductor along the  $x$  direction, the electromagnetic force will cause the electrons near the superconductor's surface to move from the ground state of zero potential positions (the white hollow circles on the left of the picture) to the excited state of high potential positions (the solid red circles on the left of the picture). As  $x$  increases, the magnetic field energy absorbed by the electrons will decay rapidly, and the displacement parameter  $\Delta(x_i)$  decreases simultaneously. When  $x > \Lambda(n, T, H_0)$ , then  $\Delta(x_i) = 0$ , the magnetic field energy disappears after being completely absorbed, and the superconductor on the right side keeps Mott insulation.

### A. Effective penetration depth

Since our theory is based on the Mott insulator model rather than the Drude model, hence the density of superconducting electrons  $n_s$  does not exist in our theory. However, under our theoretical framework, we can define the electron density  $n = 1/\Omega$ , where  $\Omega$  is the volume of a primitive unit cell of the studied superconductor. Next, we will qualitatively explain the formation mechanism of penetration depth and which physical quantities are related to it from the energy conservation and transformation perspective.

For the convenience of discussion, we still adopt the two-dimensional model of Fig. 15. When the applied external magnetic field enters the superconductor along the  $x$ -axis, it will interact with the electrons initially trapped at zero potential energy positions (indicated by the white hollow circles in the figure). These electrons will be excited to high potential energy after gaining magnetic field energy. As a direct microscopic effect on the structure, the electrons will deviate from their respective equilibrium positions along the magnetic field direction, and the  $i$ -th array electrons' displacement  $\Delta(x_i)$  is proportional to the magnetic field energy obtained by the electrons. Obviously, the magnetic field energy is converted into the potential energy of the electrons rather than being expelled from the superconductor through the development of a so-called Meissner surface current as mainstream imagined. It can also be clearly seen from this figure that the London penetration depth  $\lambda_L(n_s)$  is far less than the real value. This paper introduces the effective penetration depth (EPD)  $\Lambda(n, T, H_0)$ , which can better and comprehensively characterize the interaction process between the magnetic field and superconductor.

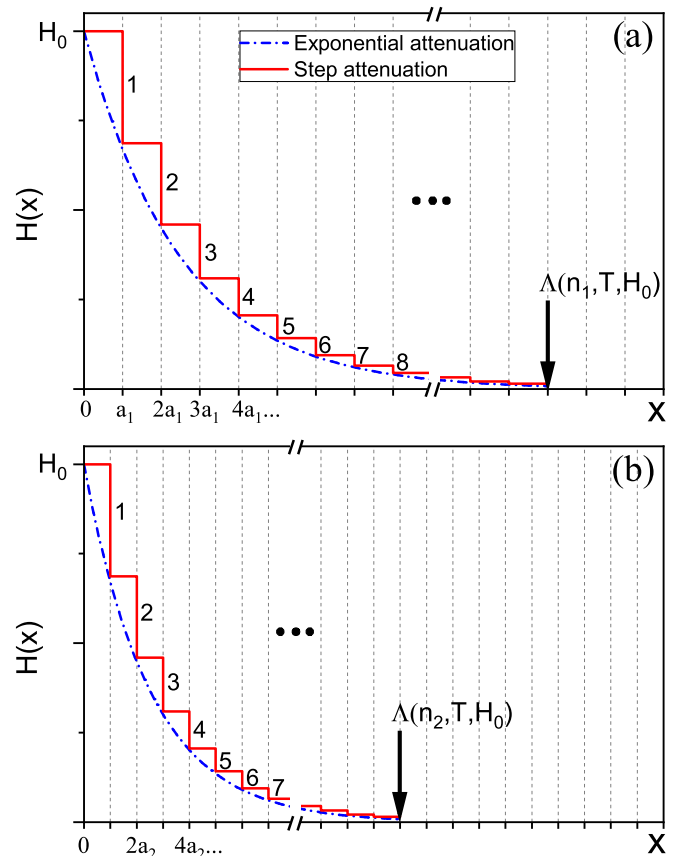


Figure 16: The quantization step of penetration depth predicted by the new theory. (a) When the electron density is low, for larger penetration depth; (b) with the increase of electron density, the penetration depth decreases.

### B. Quantized steps

In our theory, the electrons inside a superconductor are localized and form crystal structures. Hence the magnetic field entering the superconductor is not continuously absorbed but periodically. As shown in Fig. 16, the magnetic field inside the superconductor does not continuously decay as described by Eq. (15) but presents a ladder structure (quantized steps) with increasing  $x$ . The step width in the figure represents the distance between electron columns (for 3D superconductors, it represents the distance between electron layers). The step height represents the attenuation of magnetic field intensity due to the absorption of electrons, which is proportional to the number of electrons contained in the corresponding column or layer. Figs. 16(a) and (b) show the relationship between effective penetration depth  $\Lambda$  and electron density  $n$ . Suppose  $a_2 < a_1$ , then the corresponding electron density  $n_2 > n_1$ , the magnetic field energy will be absorbed faster in the latter case, so  $\Lambda(n_2, T, H_0) < \Lambda(n_1, T, H_0)$ . For three-dimensional superconducting bulk materials, various external factors, such as magnetic field strength, temperature, material size and shape, crystal defects, crystal orientation, etc., may

affect the width and height of the steps in the figure, thus affecting the EPD.

We believe that the features of a ladder structure of physical phenomena come from the localization of electrons, and the steps map the periodic structure of electrons. The quantized steps, such as the quantum Hall effect [67, 68], are prominent in two-dimensional or quasi-two-dimensional materials under extremely low temperatures and weak external fields.

### C. Superconducting magnetic levitation

As shown in Fig. 13, the EPD mainly plays a role in adjusting the net charge density near the superconducting surface where the magnetic field enters. The deeper the penetration depth, the higher the net charge density of the surface layer of the superconductor. When the penetration depth is zero, the net charge is zero because the positive and negative charges are balanced.

In the magnetic levitation experiment of Fig. 13(a), the magnetic field generated by the magnet is non-uniform, its magnitude varies with the distance and direction between the magnet and the superconductor. In other words, the microscopic penetration depth can be controlled simply by adjusting the relative position between the macroscopic magnet and the superconductor. Thereby changing the net charge density on the superconducting surface and finally realizing the automatic dynamic balance of the interaction between the superconductor and the magnet.

To explain the suspension experiment in Fig. 13(a) more intuitively, we will use the classical spring model to analyze how the superconductor automatically balances the force according to the weight of the magnet. Figure 17(a) shows a set of springs in a free state. As shown in Fig. 17(b), when an object of mass  $m$  is placed on the springs, a reaction force  $N$  is caused by the compression spring (a proper deformation  $\Delta$ ) to achieve force balance  $N = k\Delta = mg$  (where  $k$  is the spring coefficient).

As an analogy, in the absence of an external magnetic field, a superconductor in an insulating state can be simplified to a spring oscillator model, as shown in Fig. 17(c). Here note that the lateral spring oscillators are omitted from the figure. When a magnet of mass  $m$  is placed on top of the superconductor, the magnetic field will cause the “spring oscillators” to be compressed and produce a combined reaction force  $F_R$ , as shown in Fig. 17(d). The repulsive force  $F_R$  is known to be proportional to the effective penetration depth  $\Lambda(H_0)$ , where  $H_0$  represents the intensity of the magnetic field of the magnet before it enters the superconductor. Moreover, the  $H_0$  is a function of the distance  $h$  between the superconductor and the magnet. The smaller  $h$  is, the more closely they are, and the greater  $H_0(h)$  is. Hence, the force balance  $F_R = mg$  of Fig. (17) can be achieved by automatically adjusting the distance  $h$  according to the mass of the magnet. Of course, suppose the mass of the magnet is too heavy and the EPD exceeds the limit. In that case, the superconductor will undergo a phase

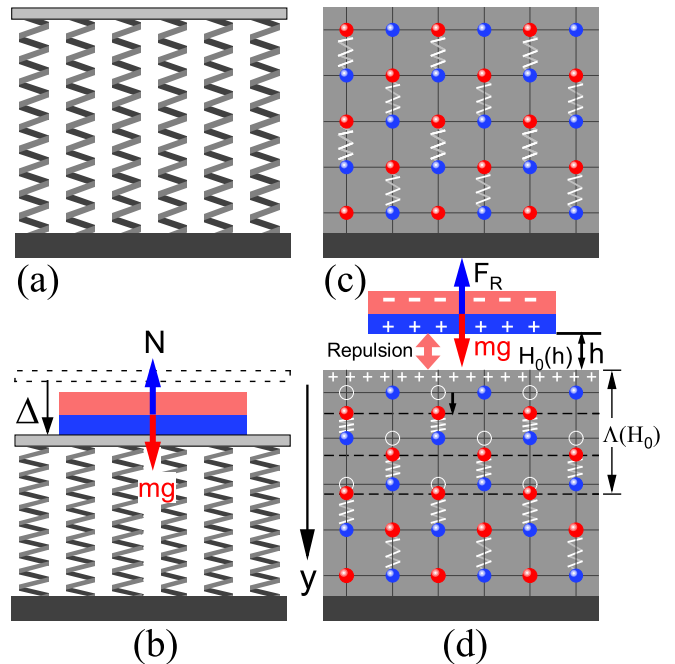


Figure 17: An analogy of superconducting levitation to a classical spring system. (a) A free spring system (assume the mass of the spring is negligible); (b) the object  $m$  achieves force balance by compressing the spring; (c) an insulating superconductor described by the “spring oscillators”; (d) similar to the classical spring system of the figure (b), the magnet suspends itself by compressing the “springs” by the magnetic field.

transition from the magnetic state to the normal state, and the levitation effect will also be destroyed.

Strictly speaking, the Meissner effect and the London penetration depth are not superconducting phenomena. They are just the low-temperature magnetization effects. By increasing the strength of the external magnetic field, which is equivalent to increasing the temperature, the electrons will gain more magnetic field energy and generate a more significant displacement. When the applied magnetic field is greater than the critical magnetic field  $H_c$  which functions as the Curie temperature of the superconductor, the magnetic state of the Meissner effect will be entirely or partially destroyed to the metallic state of Fig. 10(b) for the type-I and type-II superconductors, respectively. In the next section, we will focus on the vortex state of the type-II superconductor.

## VIII. PHYSICAL ORIGIN OF VORTEX LATTICES

Abrikosov proposed the vortex lattice in type-II superconductors in his pioneering work [40]. Since then, tremendous theoretical and experimental efforts have been directed toward understanding the behavior behind it [42–48]. However, to date, everything remains unclear at the macroscopic level. The most fundamental question of how the magnetic field leads to the formation of vortex lattices is still very chal-

lenging. What is the physical origin of the vortex state? Our theory provides new insight into the mechanisms by which vortex emerges, and why it disappears is no longer a puzzle.

### A. Vortex state with coexistence of three phases

As shown and interpreted in Fig. 18, when the superconductor is cooled below its critical temperature in an applied magnetic field  $\mathbf{H}$ , it will undergo a series of phase transitions. Depending on the magnitude of the applied magnetic field, the superconductor can transition from an insulating state to a magnetic state and from a magnetic state to a normal state or directly from an insulating state to a normal state. When  $\mathbf{H}_{c1} < \mathbf{H} < \mathbf{H}_{c2}$ , a vortex state with a mixture of insulating, magnetic, and normal tri-states is formed.

When  $\mathbf{H} = 0$ , the entire superconductor is in the Mott insulating state of Fig. 10(a). In the first-step phase transition (or the Meissner transition), when  $\mathbf{H} < \mathbf{H}_{c1}$ , the absorption of magnetic field energy by electrons induces the symmetry breaking of the proton-electron electric dipole vector, and the phase transition from the insulating state of Fig. 10(a) to the magnetic state of Fig. 10(e) or (f) occurs near the surface of the superconductor within the EPD  $\Lambda$ . In the second step, when  $\mathbf{H}_{c1} < \mathbf{H} < \mathbf{H}_{c2}$ , as the strength of the magnetic field increases, the electrons gain more energy and more significant positional perturbations, and the proton-electron electric dipole orientation order is disrupted in some tubes, where the magnetic state to normal state and insulating state to normal state phase transitions will co-occur in EPD region and inside the superconductor, respectively. Note that inside the tubes, the external magnetic field itself is not quantized. The quantized proton-electron electric dipole absorbs the magnetic field energy and then emits a magnetic flux quantum  $\Phi_0 = h/2e$ . In the third step, when  $\mathbf{H} > \mathbf{H}_{c2}$ , all electrons gain enough magnetic field energy, which leads to the destruction of the orientation order of electric dipole (or magnetic vector), and the superconductor becomes a normal metal.

In our theory, the fundamental reason for these phase transitions is the energy exchange between the magnetic field and the electrons of proton-electron electric dipoles. The occurrence of the phase transition requires the contribution of magnetic field energy. Maintaining the new phase transition state also requires a continuous energy supply from the magnetic field. Our research shows that the proton-electron electric dipole inside the superconductor absorbs the external magnetic field. This explanation differs from the conventional picture in that the magnetic field is expelled or penetrates the superconductor in the form of vortices. Furthermore, as shown in the tubes of Fig. 18, the quantized flux observed experimentally does not come from the external magnetic field but from the local quantized proton-electron pair in the tube.

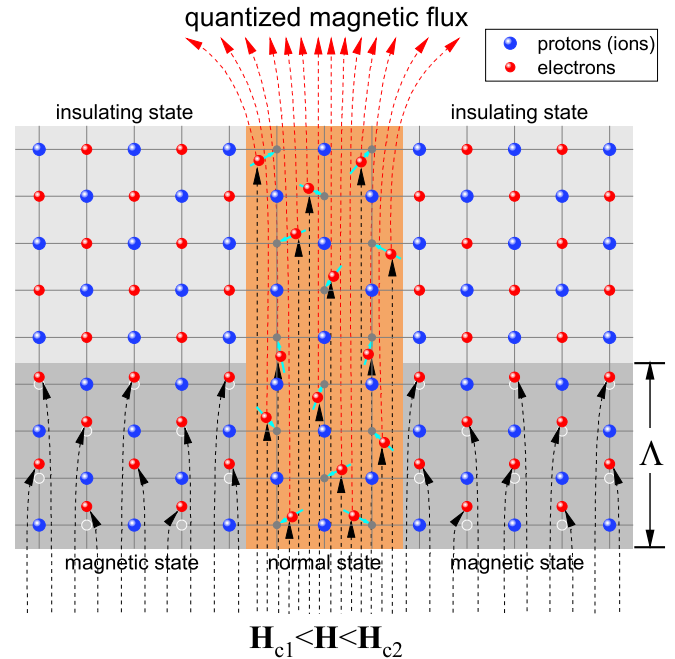


Figure 18: Microstructure of vortex state with the coexistence of three states in type-II superconductors. In the light gray region, electrons do not absorb the energy of the magnetic field and still maintain the ground state of the Mott insulation. In the gray region, electrons absorb a small amount of energy and then undergo Peierls phase transition to the Meissner magnetic state. In the orange region, the orientation order is completely disrupted after the electrons absorb enough energy.

### B. The DNA of vortex lattice

There are many experimental results for the vortex lattice structures [42–44], from which two important conclusions have been obtained. First, although the classes and structures of superconductors vary widely, their vortex lattice structures all share very similar symmetries. Second, the vortex symmetry is closely related to the orientation of the applied magnetic field. When the field is applied along the fourfold (the [001] direction), threefold (the [111] direction), or twofold (the [110] direction) symmetric axis of the superconductors, square, triangular, or distorted hexagonal vortex lattices can be observed. To the best of our knowledge, such lattice symmetry exactly matches that of *NaCl*-type lattice, as shown in Fig. 19 of a proton (ion)-electron lattice and symmetry. This figure can be considered as the DNA of the superconducting material, which determines the structure and symmetry of the vortex lattice.

It should now be apparent that the observed macroscopic perfect symmetry of the vortex lattice originates in the intrinsic microscopic perfect symmetry of the proton (ion)-electron lattice (the lattice's DNA), as shown in Fig. 20. The generation of the vortex structure still follows the principle of minimum free energy. When the vortex's symmetry matches that of the parent lattice of proton-electron pairs, the system's

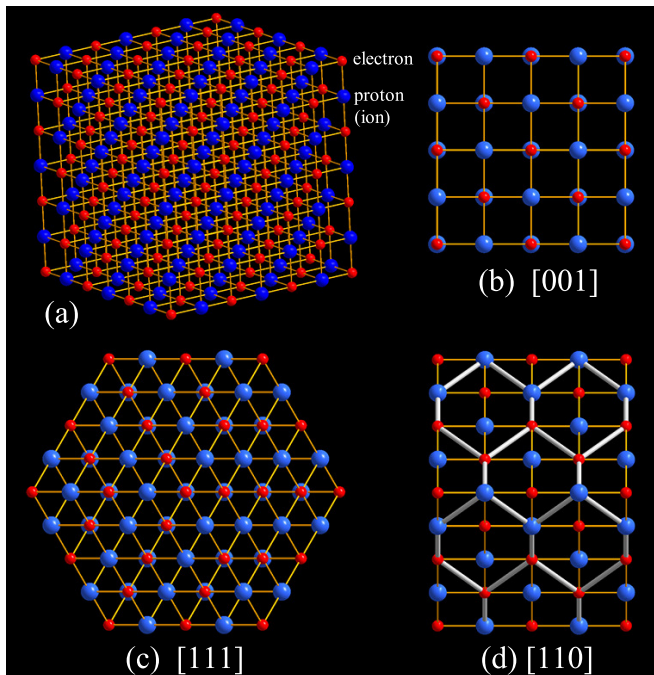


Figure 19: 3D Mott insulator, the DNA of vortex lattice. (a) A duplex lattice of proton-electron pairs with space-group  $Fm\bar{3}m$ ; (b)  $2 \times 2$  super-cells of the crystal along the fourfold [001] direction; (c) the threefold [111] direction; and (d) the twofold [110] direction, respectively. For case (d), the rectangle lattice (the thin yellow bonds) can be rearranged as a distorted hexagonal lattice (the thick light gray bonds).

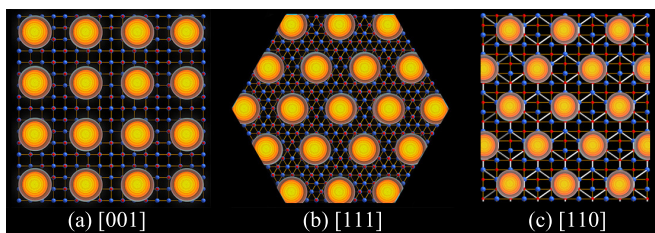


Figure 20: Matching relationship between three typical Abrikosov vortex lattices and the corresponding proton-electron electric dipole lattices. (a) A square vortex lattice in [001] direction; (b) a triangular vortex lattice in [111] direction; and (c) a distorted hexagonal vortex lattice in [110] direction.

minimum free energy and the vortex lattice's stability can be ensured. As the strength of the magnetic field increases, electrons that gain more magnetic field energy will have a more significant displacement from the equilibrium position, resulting in a strong proton-electron electric dipole interaction. This interaction will cause the orientation order of more electric dipoles to be destroyed. As a result, we can experimentally observe that the diameter and the number of the flux vortices will increase synchronously. Until the upper critical field is reached, the orientation order of the electric dipole is wholly destroyed, and the superconductor enters the normal state.

### C. Vortex dynamics

One of the most complex problems has been the explanation of the vortex dynamics in type-II superconductors [48]. The magnetic flux vortex can form various states inside the superconductor [50], such as solid, liquid, and glass [69]. Through experiments, we can observe that the magnetic flux vortex will have various forms of movement, such as hopping, creeping, and flowing. In the traditional theoretical framework, to study the movement of a vortex line, it is necessary to know the external force on the vortex line, such as the driving force, friction force, collision force, pinning force, and Magnus force. Obviously, this is a highly complex problem, and no analytical or numerical solution is possible. We wish to point out that the difficulty of this research also arises from Drude's model. The conventional theory of vortex motion is all based on the model of the random motion of carriers (electrons) in superconductors. Unfortunately, this seems wrong.

The generation of vortex lattices in superconductors requires two essential external conditions: first, a sufficiently low temperature; second, and appropriate magnetic field strength. Under low temperature and low external magnetic field, the magnetic flux lines distribute uniformly inside the superconductor. They are frozen to form an ordered lattice, as shown in Fig. 20. A type-II superconductor in a vortex state can be divided into the vortex and surrounding non-vortex regions. We here raise a question: what is the essential physical difference between the vortex and non-vortex regions? From the proton-electron pairing mechanism proposed in this paper, the electrons of proton-electron electric dipoles inside the vortex region absorb more magnetic field energy and gain higher free energy. As a result, the inner vortex is hotter than the outer vortex. This conclusion means that magnetic field or temperature instability can induce the change in the vortex region, which is the crucial physical reason for the instability and motion of the vortex lattice in the superconductor.

In the following, we will explain the vortex hopping (flowing) and creeping using Fig. 21. Figure 21(a) shows an initial vortex element of area  $A$ . Accordingly, there is a temperature field peak  $A'$  around the vortex's core, as shown by the dot-dash line in the figure below. As the temperature or magnetic field increases, the temperature and magnetic field's uniformity inside the superconductor will decrease. That is to say, there will be large random fluctuations in temperature and magnetic field inside the superconductor. Due to random fluctuations in temperature, the peak  $A'$  of the temperature field around vortex  $A$  may disappear suddenly. All the electrons inside the vortex return to equilibrium, and the vortex disappears. As shown in Fig. 21(b), almost at the same time that the peak  $A'$  disappears, a temperature peak  $B'$  may also appear suddenly in the nearby region  $B$  (the dashed line in the figure below). The higher temperature intensifies the thermal vibrations of the electrons in the region and causes them to leave their original equilibrium positions, exciting a new vortex  $B$  as shown on the right of Fig. 21(b). The vortex seems

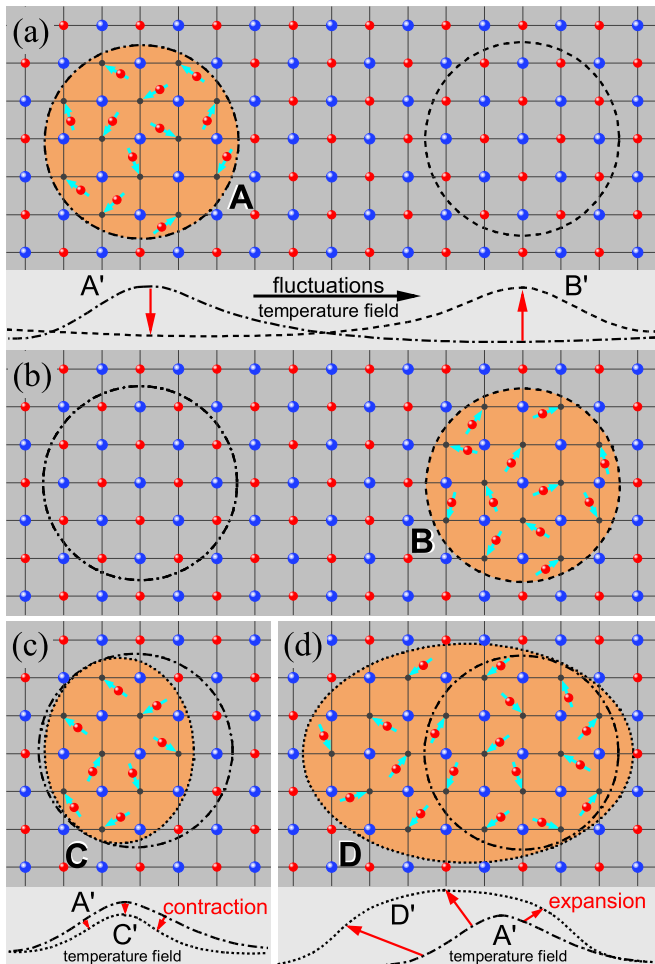


Figure 21: Top view of vortex hopping and creeping, a simple graphical explanation of vortex motion in type-II superconductors. (a) A vortex is formed in the region **A** due to the existence of the temperature field peak  $A'$  around the region, see the dot-dash line in the figure below; (b) thermal fluctuations lead to the annihilation of the temperature peak  $A'$  and corresponding vortex in region **A**, and at the same time generate new temperature peak  $B'$  and corresponding vortex in region **B**, as shown the dashed line in the figure. This process is misinterpreted as the movement (hopping) of the same vortex from **A** to **B**; (c) and (d) the vortex **A** can contract to **C** or expand to **D** in situ based on thermal fluctuations ( $A'$  to  $C'$ , or  $A'$  to  $D'$ ), often interpreted as creeping vortex dynamics.

to move (or jump) from **A** to **B** during this process. Moreover, the temperature fluctuations may occur in situ (see the dot lines  $C'$  in Figs. 21(c) and  $D'$  in Figs. 21(d) below). In this case, the vortex **A** may sometimes shrink into a thin vortex **C** of Fig. 21(c), alternatively, sometimes expand into a fat vortex **D** of Fig. 21(d), which is the experimentally observed vortex creeping.

Under our theoretical framework, it is the temperature field and the magnetic field that is moving (or changing), not the carriers (electrons) inside the vortex core, that researchers have long believed. The fundamental physical process gener-

ates and annihilates vortices by changing the superconductor's external magnetic field and temperature. Microscopically, they merely change the orientation of the proton-electron electric dipole (magnetic vector) caused by the temperature and magnetic field instability. In addition, the new theory does not require the so-called flux pinning mechanism to prevent "flux creep" in the superconductor. In the proton-electron pairing mechanism, the flux vortices in the superconductors are naturally confined and localized.

## IX. CONCLUDING REMARKS

There is a famous proverb in China called "blind people touch an elephant" which means that some people, regardless of objective conditions and constraints of personal subjectivity, make arbitrary guesses and draw conclusions based on only a one-sided understanding of things. Due to the lack of understanding of the nature of magnetism, over a hundred years, researchers have created many artificial physical concepts, such as spin, magnetic monopoles, magnetic moment, electric dipole, and magnetic dipole, which we have shown here that they all originate from the simplest proton-electron pair. It should now be clear that the electric field and magnetic field are intrinsically related. That is, isolated charges (proton or electron) generate electric fields, while paired positive and negative charges (proton-electron pair) generate magnetic fields. Remarkably, the pairing of proton and electron can achieve the perfect symmetry of Maxwell's equations. We have successfully fixed the bug of electric current that has dominated physics for over a hundred years. We have revealed that the current is Maxwell's displacement current generated by the vibration of localized electrons rather than Drude's conduction current generated by the long-range free flow of electrons that the academic community has accepted.

To test the proton-electron pairing mechanism, we have argued that the proton-electron electric dipole vector is the order parameter of the Ginzburg-Landau theory of superconducting phase transition. In this theoretical framework, many important superconducting phenomena, such as the Meissner effect, the London penetration depth, the vortex lattices, and the vortex dynamics, have been well explained by the dynamic interaction of the proton-electron electric dipole with the external magnetic field. It is worth pointing out that even below the superconducting transition temperature, a superconductor may be in five different states: an insulating state, a normal state, a metallic state, a magnetic state, or a superconducting state. The Meissner effect is the coexistence of two states (insulating and magnetic), while the vortex state is the coexistence of three states (insulating, magnetic, and metallic). Moreover, the proton-electron electric dipoles can be further self-organized into electric dipole crystals (3D Mott insulator) with space-group  $Fm\bar{3}m$  through the electromagnetic interaction, which is also the microscopic origin of the vortex lattices of type-II superconductors.

We are aware that the field of theoretical physics has been

stagnant for decades. The development of physics requires new and heretic ideas against old-established theories and models no longer valid by modern experiments. We believe the proton-electron pairing mechanism may shed new insights into all physical problems. In high-temperature cuprate superconductors, the origin of the pseudogap [70, 71], the charge stripes [72, 73], the checkerboard phases [37], the electron nematic phase [74], the magic doping [38, 39], the charge density waves (CDW) [75], etc., is controversial and still subject to debate in the condensed matter community. These debates can be perfectly settled in our theoretical framework, the studies have shown that they are related to the symmetry of the proton-electron electric dipole. Moreover, the quantum Hall effect [67, 68] and the Hall anomaly [76, 77] in superconductors are also caused by the proton-electron pair. These results will be explained in more detail in another article.

Before ending this article, it is necessary to raise an important question: why do identical proton-electron pairs, such as neutrons and hydrogen atoms, exhibit very different physical properties? This question is the greatest unresolved puzzle in physics because it involves the nature of the vacuum. As a reasonable assumption, there must be an appropriate externally supplied binding energy to bind proton and electron into a stable composite particle, which we believe the contribution comes only from the vacuum. These binding energies can be partially or wholly released under certain conditions, forming characteristic spectra for hydrogen atoms and neutrinos for neutrons. We consider photons and neutrinos to be quasi-particle modes of vacuum energy. The vacuum is not empty, which contains an infinite amount of energy and should be the consensus of the physics community.

The author would like to acknowledge Prof. Duan Feng for his invaluable suggestions and helpful discussions at the early stage of this research.

---

\* Electronic address: xiuqing\_huang@163.com

- [1] H. K. Onnes, *Leiden Comm.* **119b**, 122 (1911).  
 [2] H. G. Smith and J. O. Wilhelm, *Rev. Mod. Phys.* **7**, 237 (1935).  
 [3] J. Eisenstein, *Rev. Mod. Phys.* **26**, 277 (1954).  
 [4] J. G. Bednorz and K. A. Müller, *Z. Phys. B*, **64**, 189 (1986).  
 [5] M. K. Wu, et al., *Phys. Rev. Lett.* **58**, 908 (1987).  
 [6] M. A. Subramanian, et al., *Science* **239**, 1015 (1988).  
 [7] A. W. Sleight, *Science* **242**, 1519 (1988).  
 [8] A. W. Sleight, J. L. Gillson, and P. E. Bierstedt, *Solid State Communications* **88**, 841 (1993).  
 [9] J. Nagamatsu, et al., *Nature* **410**, 63 (2001).  
 [10] Y. Kamihara et al., *J. Am. Chem. Soc.* **130**, 3296 (2008).  
 [11] A. P. Drozdov et al., *Nature* **525**, 73 (2015).  
 [12] J. Bardeen, L. N. Cooper and J. R. Schrieffer, *Phys. Rev.* **106**, 162 (1957).  
 [13] P. W. Anderson, *Science* **235**, 1196 (1987).  
 [14] G. Baskaran and P. W. Anderson, *Phys. Rev. B* **37**, 580(R) (1988).  
 [15] J. R. Schrieffer, X. G. Wen, and S. C. Zhang *Phys. Rev. Lett.* **60**, 944 (1988).  
 [16] P. Monthoux, A. V. Balatsky, and D. Pines, *Phys. Rev. Lett.* **67**, 3448 (1991).  
 [17] E. Dagotto, *Rev. Mod. Phys.* **66**, 763 (1994).  
 [18] D. J. Van Harlingen, *Rev. Mod. Phys.* **67**, 515 (1995).  
 [19] E. Demler and S. C. Zhang, *Nature* **396**, 733 (1998).  
 [20] E. Demler, W. Hanke, and S. C. Zhang, *Rev. Mod. Phys.* **76**, 909 (2004).  
 [21] Christoph J. Halboth and Walter Metzner *Phys. Rev. Lett.* **85**, 5162 (2000).  
 [22] P. A. Lee, N. Nagaosa and X. G. Wen, *Rev. Mod. Phys.* **78**, 17 (2006).  
 [23] Adam Mann, *Nature* **475**, 280 (2011).  
 [24] P. W. Anderson, *Science* **317**, 1705 (2007).  
 [25] J. E. Hirsch, *Phys. Scr.* **80**, 035702 (2009).  
 [26] J. E. Hirsch, *Phys. Scr.* **85**, 035704 (2012).  
 [27] J. E. Hirsch, M. B. Maple and F. Marsiglio, *Physica C*, **514**, 1 (2015).  
 [28] W. Meissner and R. Ochsenfeld, *Naturwiss.* **21**, 787 (1933).  
 [29] V. L. Ginzburg and L. D. Landau, *Zh. Eksp. Teor. Fiz.* **20**, 1064 (1950).  
 [30] N. F. Mott and R. E. Peierls, in *Proc. Phys. Soc.* **49**, 72 (1937).  
 [31] J. Orenstein, and A. J. Millis, *Science* **288**, 468 (2000).  
 [32] S. M. Hayden, et al., *Nature* **429**, 531 (2004).  
 [33] H. He, et al., *Science* **295**, 1045 (2002).  
 [34] Yawen Fang, et al., *Nature Physics* **18**, 558 (2022).  
 [35] [https://www.reddit.com/r/gifs/comments/1q0d8n/the\\_meissner\\_effect/](https://www.reddit.com/r/gifs/comments/1q0d8n/the_meissner_effect/)  
 [36] F. London and H. London, *Proc. Roy. Soc.* **A149**, 71 (1935).  
 [37] T. Hanaguri, et al., *Nature*, **430**, 1001 (2004).  
 [38] S. Komiyama, H. D. Chen, S. C. Zhang, and Y. Ando, *Phys. Rev. Lett.* **94**, 207004 (2005).  
 [39] H. D. Chen, S. Capponi, F. Alet, and S. C. Zhang *Phys. Rev. B* **70**, 024516 (2004).  
 [40] A. A. Abrikosov, *Zh. Eksp. Teor. Fiz.* **32**, 1442 (1957).  
 [41] A. A. Abrikosov *Rev. Mod. Phys.* **76**, 975 (2004).  
 [42] U. Essmann, and H. Traeuble, *Phys. Lett.* **24A**, 526 (1967).  
 [43] P. L. Gammel, et al., *Phys. Rev. Lett.* **59**, 2592 (1987).  
 [44] H. F. Hess, et al., *Phys. Rev. Lett.* **62**, 214 (1989).  
 [45] G. Blatter, M. V. Feigel'man, V. B. Geshkenbein, A. I. Larkin, and V. M. Vinokur, *Rev. Mod. Phys.* **66**, 1125 (1994).  
 [46] K. Harada, O. Kamimura, H. Kasai, T. Matsuda, *Science* **274**, 1167 (1996).  
 [47] Q. Niu, P. Ao and D. J. Thouless, *Phys. Rev. Lett.* **72**, 1706 (1994).  
 [48] Y. Bugoslavsky, et al., *Nature* **410**, 63 (2001).  
 [49] H. Yang, et al., *Nature Physics*, **7**, 325 (2011).  
 [50] Mark W. Coffey and John R. Clem, *Phys. Rev. Lett.* **67**, 386 (1991).  
 [51] A. M. Campbell and J. E. Evetts, *Advances in Physics* **21**, 199 (2006).  
 [52] T. Nattermann and S. Scheidl, *Advances in Physics* **49**, 607 (2010).  
 [53] J. C. Maxwell, *Philos. Mag. J. Sci.*, London, Edinburg and Dublin, Fourth series, 161 (1861).  
 [54] G. E. Uhlenbeck and S. Goudsmit, *Nature*, **117**, 264 (1926).  
 [55] P. A. M. Dirac, *Proc. Roy. Soc. A* **133**, 60 (1931).  
 [56] P. Drude, *Annalen der Physik* **1**, 369 (1900).  
 [57] P. Drude, *Annalen der Physik* **1**, 566 (1900).  
 [58] A. Sommerfeld, *Naturwiss.* **15**, 825 (1927).  
 [59] M. Planck, *Ann. Phys.* **1**, 69 (1900).  
 [60] A. A. Michelson and E. W. Morley, *American Journal of Science* **34**, 427 (1887).  
 [61] W. Gerlach and O. Stern, *Z. Phys.* **9**, 349 (1922).  
 [62] J. E. Hirsch *Phys. Rev. B* **31**, 4403 (1985).  
 [63] C. Kim, et al., *Phys. Rev. Lett.* **77**, 4054 (1996).

- [64] A. Maeda, et al., Phys. Rev. Lett. **74**, 1202 (1995).
- [65] D. H. Wu, et al., Phys. Rev. Lett. **70**, 85 (1993).
- [66] F. Gross, Z. Phys. B, **64**, 175 (1986).
- [67] Horst L. Stormer, Rev. Mod. Phys. **71**, 875 (1999).
- [68] Yuanbo Zhang, Yan-Wen Tan, Horst L. Stormer, and Philip Kim, Nature **438**, 201 (2005).
- [69] S. A. Kivelson, E. Fradkin and V. J. Emery, Nature, **393**, 550 (1998).
- [70] Tom Timusk and Bryan Statt, Rep. Prog. Phys. **62**, 61 (1999).
- [71] H. Ding, et al., Nature **382**, 51 (1996).
- [72] S. A. Kivelson, et al., Rev. Mod. Phys. **75**, 1201 (2003).
- [73] Y. Jiang, et al., Nature **573**, 91 (2019).
- [74] M. J. Lawler, et al., Nature, **466**, 347 (2010).
- [75] G. Campi, et al., Nature, **525**, 359 (2015).
- [76] S. J. Hagen, et al., Phys. Rev. **B 41**, 11630(R) (1990).
- [77] Q. L. He, et al., Science **357**, 294 (2017).